Inorganic Chemistry

Article

pubs.acs.org/IC

Rational Design of Single-Ion Magnets and Spin Qubits Based on Mononuclear Lanthanoid Complexes

José J. Baldoví,[†] Salvador Cardona-Serra,[†] Juan M. Clemente-Juan,[†] Eugenio Coronado,*[,†] Alejandro Gaita-Ariño,*[,†] and Andrew Palii[‡]

[†]Instituto de Ciencia Molecular (ICMol), Universidad de Valencia, C/Catedrático José Beltrán 2, E-46980 Paterna, Spain

[‡]Institute of Applied Physics, Academy of Sciences of Moldova, Academy Street 5, MD 2028 Kishinev, Moldova

ABSTRACT: Here we develop a general approach to calculating the energy spectrum and the wave functions of the low-lying magnetic levels of a lanthanoid ion submitted to the crystal field created by the surrounding ligands. This model allows us to propose general criteria for the rational design of new mononuclear lanthanoid complexes behaving as single-molecule magnets (SMMs) or acting as robust spin qubits. Three typical environments exhibited by these metal complexes are considered, namely, (a) square antiprism, (b) triangular dodecahedron, and (c) trigonal prism. The developed model is used to explain the properties of some representative examples showing these geometries. Key questions in this area, such as the chemical tailoring of the superparamagnetic energy barrier, tunneling gap, or spin relaxation time, are discussed. Finally, in order to take into account delocalization and/or covalent effects of the ligands, this point-charge model is complemented with ab initio calculations, which provide accurate information on the charge distribution around the metal, allowing for an explanation of the SMM behavior displayed by some sandwich-type organometallic compounds.

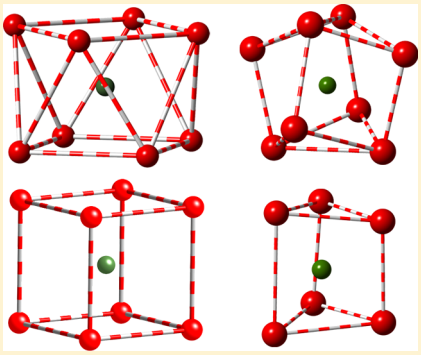

INTRODUCTION

For more than 15 years, single-molecule magnets (SMMs) have been a hot topic in molecular magnetism because of their rich physical behavior. Thus, crystals of these molecules exhibit a superparamagnetic blocking at T_B, characterized by slow relaxation of the magnetization at lower temperatures and by magnetic hysteresis.[1,2] On the other hand, they are among the most complex magnetic entities that show quantum phenomena like quantum tunneling of the magnetization,[3] quantum coherence, or quantum interference, and thus they have been postulated as candidates for spin qubits in quantum computing.[4]

The first generation of SMMs was based on polynuclear magnetic complexes (magnetic clusters) with strong magnetic coupling between d transition-metal ions, leading to a high-spin ground state, S, well separated in energy from the excited spin multiplets, and a negative uniaxial anisotropy, D, which causes a splitting of this ground state into $\pm S_z$ sublevels and creates a barrier for the spin reversal.[5] The major synthetic challenge in this case was to increase this energy barrier and, consequently, the blocking temperature T_B, by designing molecules having maximum values of S and D. However, the success of this approach has been very limited, as demonstrated by the fact that the first SMM, the so-called Mn_{12}, is still among the systems exhibiting the highest effective barriers (ca. 45−50 cm^{-1}) and hysteresis up to 4 K. More recently, magnetic clusters containing highly anisotropic lanthanoid ions have also been synthesized.[6] These complexes have shown effective barriers as high as 100 cm^{-1} and hysteresis up to 8 K.

In the past few years, a new generation of SMMs have appeared with the discovery that a mononuclear complex formed by a single magnetic center coordinated to ligands, usually an anisotropic lanthanoid ion, may also behave as a SMM. These compounds are known as single-ion magnets (SIMs) or mononuclear SMMs.[7] The first example of a molecular SIM was reported by Ishikawa et al. in 2003 in complexes of the general formula $[LnPc_2]^-$, with a "double-decker" structure and phthalocyanines as ligands.[8] Thus, the antiprismatic D_{4d} crystal field (CF) induced by the octacoordinated atoms around the Ln^{3+} ion splits its ground magnetic state, characterized by the total angular momentum, J, into $\pm M_J$ sublevels. In some cases, this leads to a sublevel scheme in which the levels with the higher $|M_J|$ values are stabilized with respect to the levels with the lower $|M_J|$ values. This creates a barrier that explains the SMM behavior observed in the terbium derivative for which the ground-state magnetic doublet corresponds to that with the maximum M_J value (=±6), being separated from the first excited level (M_J = ±5) by more than 300 cm^{-1}.

Later on, in 2008 our group showed that the concept of SIMs can be extended to other families of mononuclear lanthanide complexes. Thus, we discovered that polyoxometalate (POM) complexes encapsulating a lanthanoid ion do also exhibit SMM behavior for coordination sites close to the antiprismatic D_{4d} symmetry.[9] In this case, the different distortion of the

Received: September 24, 2012
Published: October 26, 2012

   dx.doi.org/10.1021/ic302068c | *Inorg. Chem.* 2012, 51, 12565−12574

antiprismatic site (axially compressed) compared to that shown by the $[LnPc_2]^-$ complexes (axially elongated) leads to a different splitting of the $\pm M_J$ levels. Thus, under this CF, the higher M_J values ($\pm^{13}/_2$) are stabilized in the erbium derivative, which behaves as a SMM, while in the terbium derivative, M_J = 0 is a ground state and the level with $M_J = \pm 6$ corresponds to an excited state; hence, it does not behave as a SMM.

Since then, many examples of mononuclear lanthanide complexes having different coordination geometries and different types of ligands have also shown SMM properties, thus demonstrating that the SIM concept is quite general. Some relevant examples are the organometallic double-decker Er^{3+} compound[10] and the acetylacetonate lanthanoid complexes,[11] both studied by Gao et al., and the DyDOTA complex reported by Sessoli et al.[12] In addition, some SIMs based on mononuclear uranium complexes have been reported.[13] Finally, mononuclear d transition metals have also shown to behave as SIMs, with the iron pyrrolide molecules[14] and a $Co(SPh)_4$ salt[15] being the most quoted cases. Note that the concept of SIMs is not restricted to the molecular world. In fact, the family of lanthanoid-substituted scheelites of the formulas $LiY_{1-x}Ho_xF_4$ and $Ca_{1-x}Er_xWO_4$ has also provided examples of SIMs. Thus, the former system behaves as a SMM showing a staircase-like hysteresis loop of the magnetization due to a nuclear-spin-driven quantum relaxation,[16] while the latter behaves as a spin qubit exhibiting coherent Rabi oscillations, which are indicative of high quantum coherence.[17]

The present work has been motivated by the need to find general criteria for the rational design of new mononuclear lanthanoid complexes behaving as SMMs or acting as spin qubits. Often, the same nanomagnet may be regarded as either a SMM or a molecular spin qubit, depending on the experiment performed. Still, some differences between these two aspects exist. Thus, the magnetization orientation of a molecule is utterly described by a classical bit. Instead, if we consider the molecule as a qubit, one additionally needs to address arbitrary superpositions between quantum states.

Nevertheless, in both cases, the final goal is to manipulate the quantum dynamics of a small number of levels, and in this regard, one needs the following:

(1) To know the mixing within our target subset of levels. This knowledge is required for the design of the system and, subsequently, for manipulation of the spin dynamics.

(2) To guarantee an effective isolation of the ground state from the rest of the spectrum, in the form of a large energy gap. Moreover, the optical, electric, or magnetic operations that one can perform on this subsystem should not cause leakage to excited states.

Previously, a qualitative approach to predicting the ligand disposition to obtain SMMs has been reported.[18] Here we will develop a general theoretical approach to calculating the energy spectrum and the wave functions of the low-lying magnetic levels of a lanthanoid ion submitted to the CF created by the surrounding ligands. We show that this model can allow us to predict which lanthanoids and geometries are more suited for obtaining SMMs or robust spin qubits. Key questions in this area, such as the chemical tailoring of the physical properties of these nanomagnets (superparamagnetic energy barrier, tunneling gap, spin relaxation time, etc.), are discussed. The computational approach, initially based on a point-charge model, can also incorporate delocalization and/or covalent effects of the ligands through ab initio calculations that give accurate information on the charge distribution around the metal.

RESULTS AND DISCUSSION

In a first approximation, a mononuclear lanthanoid-based complex will behave as a SMM, i.e., it will have a superparamagnetic energy barrier, if splitting of the ground state of the lanthanoid, J, caused by the CF created by the ligands is such that the ground-state magnetic doublet has a high M_J value, $\pm M_J$, which is well separated in energy from the excited-state M_J sublevels. Such a splitting will be dependent on the lanthanoid and on the symmetry and distortion of the coordination environment. The theoretical background of the CF calculation and the computational method will be presented in a separate section.

As far as the lanthanoid is concerned, we notice that J and the Stevens coefficients (α, β, and γ)[19] are fixed and are specific for each lanthanoid. It is obvious that the first condition to get a high-M_J ground-state doublet is to have a large J value. Hence, we should focus on the second half of the lanthanoid series because these ions possess a negative spin−orbit coupling, which stabilizes the states with maximum J values ($J = L + S$). According to this, Tb^{3+}, Dy^{3+}, Ho^{3+}, Er^{3+}, and Tm^{3+} will be the best choices, with Yb^{3+}, Pr^{3+}, and Nd^{3+} coming next.

The nuclear spin of the lanthanoid can also be relevant because it will determine the shape of the hysteresis loop, including whether there is quantum tunneling of the magnetization at zero field.[20]

As far as the coordination environment is concerned, the first condition for designing SIMs will be to have highly symmetric axial sites because they often provide the most favorable case to have pure M_J wave functions. The level splitting produced by strong diagonal terms can avoid the mixture with low M_J states even for nonideal geometries. Neglecting high-order parameters, one can expect that α-negative lanthanoids (Tb^{3+}, Dy^{3+}, Ho^{3+}, Pr^{3+}, and Nd^{3+}) will stabilize a high-M_J ground-state doublet when they are in an axially elongated coordination environment, whereas α-positive lanthanoids (Er^{3+}, Tm^{3+}, and Yb^{3+}) will need equatorial or axially compressed coordination environments to achieve this. This can be easily understood if we notice that the B_2^0 parameter is proportional to the axial zero-field-splitting parameter (D) and related to the A_2^0 parameter by the following expression: $B_2^0 = D/3 = \alpha\langle r^2\rangle A_2^0$. Thus, a negative B_2^0 will require a negative α (because A_2^0 is positive) for an elongation or a positive α for a compression (because in this case A_2^0 is negative). Finally, for particular symmetries where B_2^0 does not dominate (e.g., octahedral coordination geometry), the higher-order B_4^0 parameter usually does. In these cases, to favor stabilization of the medium-to-high M_J compared with the lowest M_J states, β-positive lanthanoids (Tb^{3+}, Er^{3+}, and Tm^{3+}) should have ligands on the z axis and/or on the xy plane, whereas β-negative lanthanoids (Pr^{3+}, Nd^{3+}, Dy^{3+}, Ho^{3+}, and Yb^{3+}) should have them at polar angles of around 50−60°. These behaviors are perhaps more easily understood through analysis of Figure 2.

In the following, we will study in detail the influence of the coordination environment on the splitting of the J ground state of the lanthanoid complex in three typical cases, namely, the (a) square antiprism, (b) triangular dodecahedron, and (c) trigonal prism. We will first assume both ideal and real structures to discuss the effect of these CFs and to give some general guidelines for the choice of the most adequate geometry.

dx.doi.org/10.1021/ic302068c | Inorg. Chem. 2012, 51, 12565−12574

a. Square-Antiprismatic versus Cubic Geometry. Herein, we compare the well-known square-antiprismatic geometry (D_{4d} ideal symmetry) and the cubic geometry (O_h ideal symmetry). POM chemistry provides nice examples of these two octacoordinated environments (Figure 1). In fact,

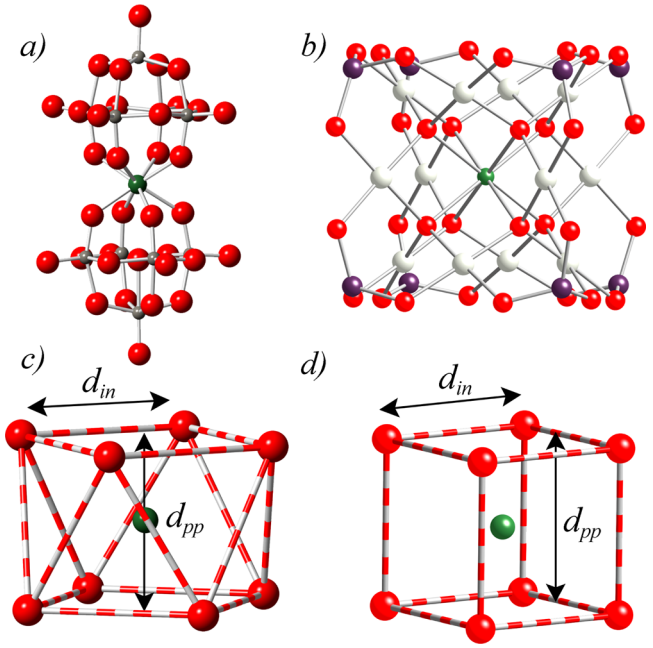

Figure 1. Schematic structures of two different POM complexes with interesting coordination symmetry, (a) **1** and (b) **2**, and their coordination polyhedra, (c) square antiprism and (d) cube. The d_{pp} parameter defines the average distance between the two oxygen-based square planes. d_{in} is the average O−O distance within the oxygen-based square planes.

these molecular metal oxides have rigid and stable structures that can impose highly symmetric CFs to the lanthanoid. In Figure 1, the structure of the square antiprism $[Ln(W_5O_{18})_2]^{9-}$ (**1**) is compared to the cubic structure of $[LnPd^{II}_{12}(As^{V}Ph)_8O_{32}]^{5-}$ (**2**) recently reported by Kortz et al.[21] Experimentally, the magnetic behavior of these two series shows that while for **1** some derivatives exhibit a SMM behavior, for **2** all of the derivatives exhibit a fast spin relaxation at low temperatures.[22] It seems therefore that the D_{4d} symmetry is more suitable for the design of SIMs than the O_h symmetry is.

Let us now discuss the origin of such a difference. The real geometry for the erbium derivative of the series **1** is plotted in Figure 1. In this compound, the ratio between the interplanar distance d_{pp} = 2.47(1) Å (calculated as the distance between the upper and lower planes containing the four oxygen atoms) and the average distance between the four neighboring oxygen atoms placed in each plane, d_{in} = 2.86(5) Å, is indicative of an axial compression of the square antiprism. Using this geometry, the main CF parameters to be considered are B^0_2, B^0_4, and B^0_6 (those allowed by an ideal D_{4d} system), but because of distortion of the site, nonnegligible values for B^3_4, B^4_4, and B^4_6 appear. The calculations lead to an isolated ground-state doublet, corresponding to that with the highest M_J value ($\pm^{15}/_2$), which is separated in energy from the first excited-state doublet $M_J = \pm^{13}/_2$ by 56.8 cm^{-1}. Such a feature explains the SMM behavior exhibited by this erbium compound. In fact, the energy gap between the ground state and the first excited state is close to the effective energy barrier determined experimentally (38.1 cm^{-1}). This indicates that relaxation will take place by quantum tunneling through the first excited state because the corresponding wave function is formed by a mixture of the $M_J = \pm^{13}/_2$ function and those having $M_J = \pm^{1}/_2$ and $\pm^{3}/_2$. Notice that, in this simple description, other factors, such as the presence of phonons or the effect of other nuclei, which are supposed to modify the effective barrier, have been neglected.

Experimental CF parameters can be obtained from the magnetic properties following the Ishikawa procedure.[23] For an isomorphic series of lanthanoid complexes, the CF parameters could be determined by a simultaneous fit of all of the $\chi_m T$ values under the assumption that each CF parameter shows a linear variation from the f^8 (Tb^{3+}) system to the f^{13} (Yb^{3+}) system.

This theoretical CF model can be extended to other lanthanoid derivatives of **1**, such as Ho^{3+}, Tb^{3+}, and Dy^{3+}. In this axially compressed geometry, both the erbium and holmium derivatives have high-spin ground states. Thus, they are both more likely SIM candidates than terbium and dysprosium, in contrast with the Pc_2Ln case. Nevertheless, according to our calculations summarized in Table 1,

Table 1. Calculated Low-Lying Energy Levels and Eigenvector Contributions with C_I^2 > 5% For $[Ln(W_5O_{18})_2]^{9-}$ (1; Ln = Er^{3+} and Ho^{3+}, up and down, Respectively)

energy (cm^{-1})	c_i^2 (M_J)
0.00	0.9996 ($-^{15}/_2$)
0.00	0.9996 ($^{15}/_2$)
56.82	0.9975 ($-^{13}/_2$)
56.82	0.9975 ($^{13}/_2$)
103.45	0.9316 ($-^{1}/_2$)
103.45	0.9316 ($^{1}/_2$)
energy (cm^{-1})	c_i^2 (M_J)
0.00	0.453 (−4), 0.453 (4)
0.11	0.451 (−4), 0.451 (4)
12.22	0.273 (−5), 0.217 (−3), 0.216 (3), 0.273 (5)
12.41	0.284 (−5), 0.205 (−3), 0.205 (3), 0.285 (5)
16.93	0.186 (−5), 0.249 (−3), 0.249 (3), 0.186 (5)
17.50	0.160 (−5), 0.284 (−3), 0.284 (3), 0.160 (5)

comparable minor deviations from the ideal geometry have markedly different effects on the erbium and holmium systems: the erbium derivative preserves a 99.96% purity of the (well-isolated) $M_J = \pm^{15}/_2$ ground state, while the holmium complex displays a thorough mixing, both in the ground state and in the low-lying excited states. This can be linked to the experimental behavior: for $[Er(W_5O_{18})_2]^{9-}$, the superparamagnetic blocking happens for frequencies as low as 100 Hz, while for $[Ho(W_5O_{18})_2]^{9-}$, the out-of-phase susceptibility only begins to arise at frequencies on the order of 10 kHz.

An important feature of these results is the sign of B^0_2, which is positive in Tb^{3+}, Dy^{3+}, and Ho^{3+} and negative for Er^{3+}. In general, the sign of B^0_2 for a given lanthanoid is determined by the combination of the axial ($\theta < 54.7°$) or equatorial character ($\theta > 54.7°$) of the sites, as defined by the ligand position. In fact, from Figure 2, it is easy to understand that at $\theta \approx 54.7°$, which corresponds to an axially nondistorted antiprism (defined by $d_{in} = d_{pp}$) or to a cube, a point charge is on a

dx.doi.org/10.1021/ic302068c | Inorg. Chem. 2012, 51, 12565−12574

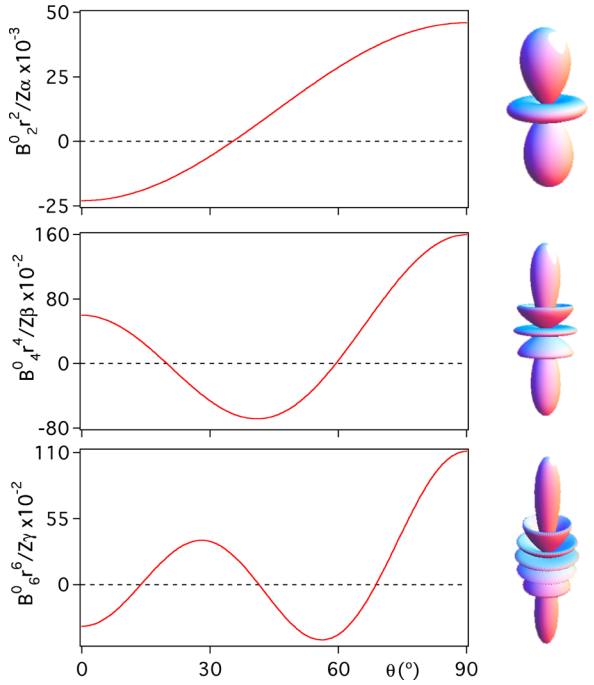

Figure 2. Magnetostructural correlation of B^0_2/α, B^0_4/β, and B^0_6/γ with the θ polar angle in the case of D_{4d}. Right side: shapes of Y_{20}, Y_{40}, and Y_{60}; in Y_{20}, one can recognize the shape of the d_{z^2} orbital.

node, so that it contributes to B^0_4 and B^0_6, while B^0_2 is equal to zero.

An example with cubic symmetry is provided by the series **2**. Calculations performed on the Er^{3+} derivative using real coordinates show a mixed ground-state doublet, with the most important contribution being that of $M_J = \pm^1/_2$, followed by $\mp^{15}/_2$, $\mp^7/_2$, and $\pm^9/_2$. The first 4-fold degenerate excited state is located at 13.5 cm^{-1}, where the majority of the M_J values are contributing to the wave function. This low extensive mixing of the sublevels yields a fast quantum tunneling of the magnetization. On the other hand, the presence of $\pm^1/_2$ in the ground state explains why this molecule does not possess SIM behavior. Because of the well-known relations for cubic symmetry, $B^4_4/B^0_4 = 5$ and $B^4_6/B^0_6 = -21$, this system may be defined only by two CF parameters, B^0_4 and B^0_6. The absence of B^0_2 (meaning $D = 0$) reduces the possibilities of using a different lanthanoid (e.g., Tb^{3+}, Dy^{3+}, or Ho^{3+}) to obtain a higher barrier. In conclusion, D_{4d} symmetry (axially elongated for Tb^{3+}, Dy^{3+}, or Ho^{3+} or equatorially compressed for Er^{3+}) is much more favorable than cubic (O_h) symmetry for obtaining slow relaxation of the magnetization. This is better understood by performing a magnetostructural study in which the D_{4d} symmetry is taken as a distorted case of the O_h symmetry when the two squares are staggered rather than eclipsed. This situation is defined by the torsion angle between the upper and lower squares, φ, which goes from 0° in the O_h symmetry to 45° in the D_{4d} symmetry. To perform this calculation, the coordinates of the four point charges forming a square are rotated with respect to that of the other square around the z axis. A typical distortion of the D_{4d} symmetry can be obtained by slightly deviating φ from 45° (see Figure 3, left). The calculations indicate that the CF parameters B^0_4 and B^0_6 are invariant with respect to φ. Additionally, B^4_4 and B^4_6 are nonzero, except for $\varphi = 45°$, evolving as a function of φ (Figure 3, right). Thus, exact cancelation of these two parameters occurs for the

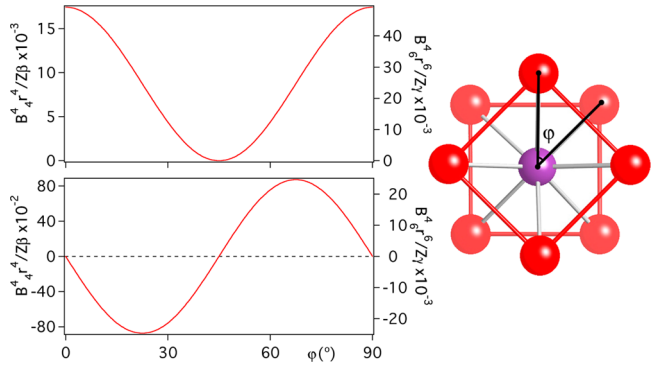

Figure 3. (left) Magnetostructural correlation of the real (top) and imaginary (down) parts of B^4_4/β and B^4_6/γ with φ. (right) Scheme depicting the torsion angle that describes the rotation of a cube from O_h to D_{4d} symmetries.

D_{4d} symmetry, while the maximum values are reached for the O_h one. In conclusion, one can anticipate that for an ideal D_{4d} symmetry the wave functions will be described by pure $\pm M_J$ values, while for a cubic symmetry, the presence of the B^4_4 and B^4_6 CF parameters will result in an extensive mixing of functions with different M_J values (in particular, those differing by $\Delta M_J = 4$). On the other hand, as we have seen before, the B^0_2 parameter will be zero either for a cubic symmetry or for a nondistorted antiprismatic symmetry. This is the key parameter for creating a gap between the M_J ground-state doublet, and the excited states (and therefore a barrier) will only appear by axial distortion of the antiprism (elongation or compression). Using such a procedure, one is able to analyze real structures that are between these two symmetries, as determined by shape analysis.[24]

b. Triangular Dodecahedron. A triangular dodecahedron presents D_{2d} symmetry (Figure 4), closely related to S_4, with a

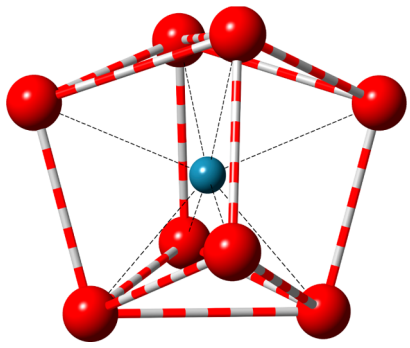

Figure 4. Schematic structure of a triangular dodecahedron site with D_{2d} symmetry, with 'axial' and 'equatorial' ligands.

coordination number of 8 around the lanthanoid ion. In this case, the most important examples are found in the salts $LiHo_xY_{1-x}F_4$ and $Er_xCa_{1-x}WO_4$, both showing a scheelite structure, with tetragonal distortion from the cubic symmetry arising from the displacement of two opposite edges in opposite directions. This yields a symmetry reduction from O_h to S_4. As a real example for this coordination symmetry, we have used the $LiHo_xY_{1-x}F_4$ compound, obtaining the following CF terms: B^0_2, B^0_4, B^0_6, B^3_4, B^4_4, and B^4_6. Because of the ionic character of F ions, this system provides an excellent scenario to test the point-charge model. The calculated splitting diagram for the $J = 8$ ground state of Ho^{3+} in this environment reveals a

dx.doi.org/10.1021/ic302068c | Inorg. Chem. 2012, 51, 12565−12574

ground-state doublet defined by two functions composed by the following M_J values: (+7, +3, −1, −5) and (−7, −3, +1, +5). Notice that, even if these two functions are formed by an extensive mixture of M_J, they cannot exhibit any tunneling because they do not present any overlap. On the contrary, the first excited-state doublet (lying at 10.8 cm^{-1} above the ground-state doublet) is formed by two functions composed by (+6, +2, −2, −6) and (−6, −2, +2, +6); these are mixed because both contain the same M_J values but different coefficients for the linear combination, thus allowing for tunneling. According to this, spin relaxation will take place by tunneling within the first excited-state doublet, but not within the ground state, explaining why this compound exhibits SMM behavior.

Notice that the extensive mixture of M_J calculated in the present case is a consequence of the presence of nonnegligible extradiagonal parameters B_4^4 and B_6^4. In particular, B_4^4 and B_6^4 parameters are 1 and 2 orders of magnitude larger than the corresponding diagonal terms (B_4^0 and B_6^0), respectively.[25] These ratios are even higher than those of cubic geometry. Figure 5 can be useful to understand the variation of these

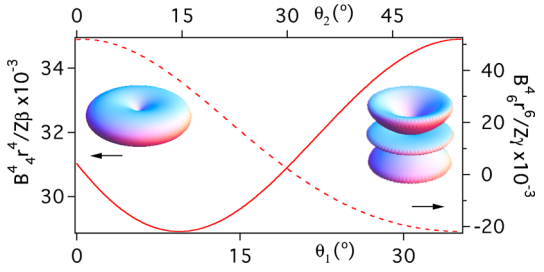

Figure 5. Variation of B_4^4/β and B_6^4/β for eight ligands submitted to a continuous D_{2d} distortion between an octahedron (left) and a cube (right). The four 'axial' ligands (see Figure 4) deviate from their initial positions at the z axis reaching the cubic disposition at $\theta_2 = 54.74°$, while the four 'equatorial' ligands leave the plane and complete the cube at $\theta_1 = 35.26°$. Insets: shapes of Y_{44} and Y_{64}.

extradiagonal parameters. As can be seen there, B_4^4 is almost constant for any degree of D_{2d} deformation between an ideal cube and an octahedron. For large deformations, B_6^4 can even suffer a sign reversal, but for realistic deformations (i.e., on the order of 15°), it is fairly stable. In contrast, both B_4^0 and B_6^0 display nodes in this region of intermediate angles (Figure 2), so moderate deformations can be expected to affect them more drastically.

c. Trigonal Prism. Trigonal prisms abound in lanthanoid coordination chemistry, either bare or with up to three apexes in the center of the rectangular faces. Some complexes having these kinds of coordination sites exhibit SMM behavior (Figure 6). This is the case of $[Tb(picNN)_3]$ (**3**),[26] where picNN = picolinate-based nitronylnitroxide, $[Dy_2(hfac)_6(H_2O)_2(L)]$ (**4**),[27] where hfac = 1,1,1,5,5,5-hexafluoroacetylacetonate anion and L = 4,4′,7,7′-tetra-*tert*-butyl-2,2′-bis(1,3-benzodithiole)-5,5′,6,6′-tetrone, and $[Ln(FTA)_3L]$ (**5**),[28] where FTA = 2-furyltrifluoroacetonate and L = *S*,*S*-2,2′-bis(4-benzyl-2-oxazoline).

It has to be remarked that, for these low-symmetry highly distorted geometries (often seen as distorted D_{4d} complexes), this result is not easy to predict. In any case, if one intends to approach this problem as a rational design process, one should first take into account that an ideal trigonal prism (D_{3h} symmetry) can only present B_2^0, B_4^0, B_6^0, and B_6^6 terms. The presence of the extradiagonal CF parameter B_6^6 means mixing between M_J values differing by ±6. It is crucial to note that this will produce direct tunneling only for doublets involving states with $M_J = \pm 3$ or ±6, and even in these cases, the compound may show SMM behavior if B_2^0 is large enough. This seems to be the case for the derivative **3**, where slow relaxarion of the magnetization has been exhibited, including magnetic hysteresis under 1 K.[25] Preliminary calculations have shown an $M_J = \pm 6$ ground-state doublet, which is clearly separated (around 200 cm^{-1}) with respect to the nearest excited-state doublet ($M_J = \pm 5$), in good agreement with the experiment. Another prediction is that for half-integer spins like Nd^{3+}, Sm^{3+}, Dy^{3+}, Er^{3+}, and Yb^{3+}, an ideal D_{3h} coordination symmetry may be as good as a pseudoaxial one for getting SMM behavior. In fact, even though actinoids cannot be precisely described by the Russell−Saunders scheme like lanthanoids, examples of U^{3+} ($J = {}^9/_2$) in this coordination environment have recently shown SMM properties.[29] The method reported in this work has recently been applied to describe such systems.[30]

Covalent Effects. Many-body effects that modify the simplest ionic picture are usually grouped under the catch-all term "covalent effects".[30] For simple halides, oxides, and other markedly ionic ligands, covalent effects are negligible and CF can be reproduced by simply substituting each atom in the coordination sphere by a point charge. In other molecules, where this assumption is no longer adequate, the point-charge model should be refined to include at least the effects of polarization and deformation of the electron clouds. In a first step, the use of partial charges, distributed among a larger number of centers and calculated by density functional theory (DFT), can account for some of these effects.

As an illustrative example, we have chosen the compound $[Dy^{III}(COT'')_2Li(THF)(DME)]$ [COT″ = 1,4-bis(trimethylsilyl)cyclooctatetraenyl dianion, THF = tetrahydrofuran, and DME = dimethyl ether], which has recently been reported to display SMM behavior.[22] This sandwich-type compound contains the metal complex $[Dy^{III}(COT'')_2]^-$ (Figure 7, right). It is clear that in this case the assumption of a purely ionic model, with a negative charge on each carbon atom, is totally unrealistic. In order to use the CF model, first, we have calculated the electronic density of an idealized COT ligand through DFT [Becke3LYP/6-31G(d)]. This calculation has provided the effective partial charges of the carbon ($q_1 = -0.175$) and hydrogen ($q_2 = -0.0742$) atoms on this ligand. Second, we have introduced these charges in the CF calculation code in order get the CF parameters. The distances $r_1 = 0.950$ Å, $r_2 = 1.415$ Å, and $r_3 = 3.794$ Å have been averaged from the crystallographic data. Using r_1, r_2, r_3, q_1, and q_2, we have obtained $B_2^0 = -15.3$ cm^{-1}, $B_4^0 = 3.31 \times 10^{-2}$ cm^{-1}, and $B_6^0 = -8.23 \times 10^{-5}$ cm^{-1}. The resulting energy-level scheme displays a high-spin M_J doublet = $\pm{}^{15}/_2$ as the ground state, with the first excited-state sublevel lying at 244 cm^{-1}, thus explaining the SMM properties.

Further improvements on the point-charge model reported here are easily conceivable. For instance, instead of a single charge centered on each nucleus, a larger number of smaller charges can be distributed around each atom. In this way, the actual electronic shape of the ligands can be mimicked. This extension allows us to consider the proper location of lone pairs and π clouds and to distinguish between markedly different anionic radii. Another possible refinement is to modify the coordinates of the partial charges to account for the coordination bond.[51] Such a treatment of the covalence effects was successfully used by us for the theoretical study of a d

dx.doi.org/10.1021/ic302068c | *Inorg. Chem.* 2012, 51, 12565−12574

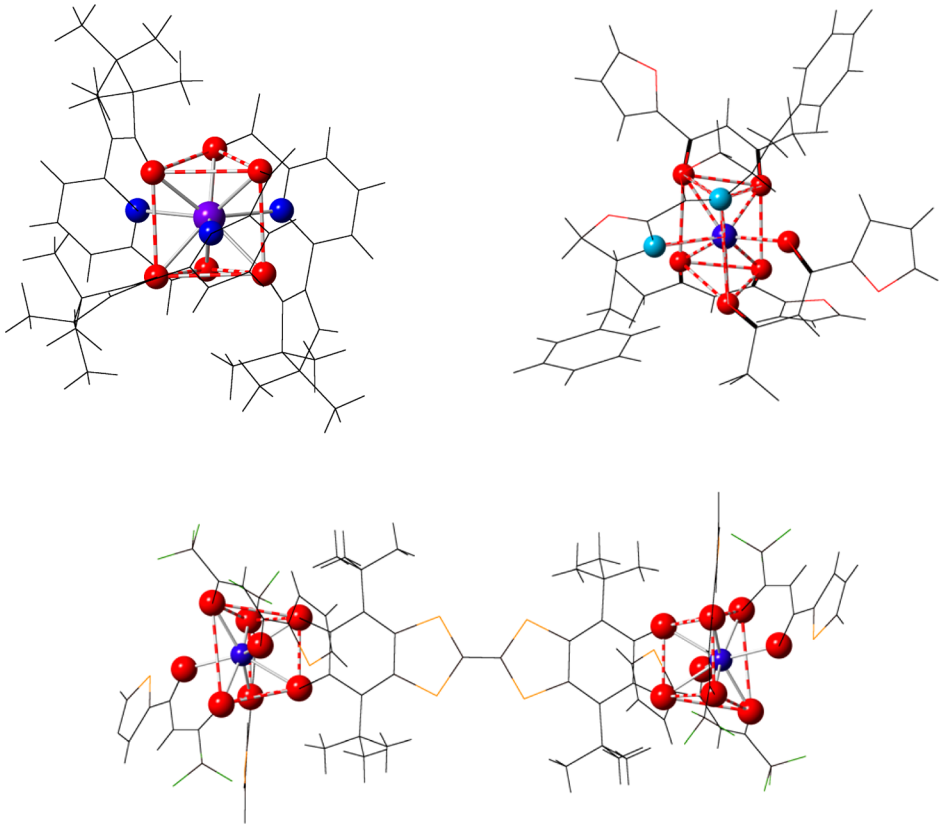

Figure 6. Structures of mononuclear lanthanoid complexes close to a trigonal prism that display SMM behavior: (top left) **3**; (top right) **4**; (bottom) **5**.

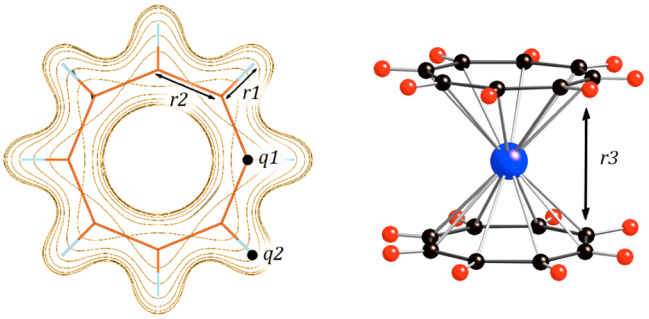

Figure 7. Left: Electronic density of COT calculated by DFT methods. Right: Idealized structure for a $Dy(COT'')_2$ sandwich.

transition-metal SIM[31] and is somewhat similar to the effective-charge model proposed by Morrison.[32] An alternative possibility to taking into account the covalent effects is to apply the so-called "exchange-charge model".[33]

Remarks for the Design of Spin Qubits. Some special considerations need to be taken into account when designing a lanthanoid complex for its use as a spin qubit instead of just as a SIM, which mainly depend on (i) its nuclear spin, (ii) its tunneling gap, and (iii) its environment.

The first issue is the isotopic purity of the lanthanoid. At the very least, that is desirable and a need in most cases. Like a badly purified product, a sample with a natural distribution of isotopes contains a random mixture of quantum systems. In that sense, holmium, terbium, thulium, and praseodymium are especially adequate in this context because they only have one stable isotope each. Note that a nuclear spin accessible through contact hyperfine interaction has proven to be a very valuable resource because it can provide access to a larger number of well-defined states.[34] Nuclear spins are also of dramatic importance in determining the parity of the system, i.e., whether the ion is Kramers or non-Kramers. Elements with an even atomic number, like dysprosium, erbium, ytterbium, and neodymium, have half-integer J and some of their isotopes are $I = 0$, therefore being Kramers ions. In those cases, ligand-field extradiagonal parameters will potentially mix, but will not split, the components of the ground-state doublet. Hence, in those cases in which a degeneracy of the states is required, the best choice will be to use Kramers ions, while if a splitting is needed, non-Kramers ions will be preferred.

As a second consideration, the tunneling gap Δ in the ground state is critical for manipulation of the quantum state. Large tunneling gaps can be advantageous both for an easier spin manipulation[35] and for diminishing decoherence. In that sense, mononuclear lanthanoid-based qubits/SIMs (with gaps up to $\Delta = 0.1-1$ cm^{-1}) are vastly superior to cluster-type transition-metal-based SMMs (with the usual gaps in the range of $\Delta = 10^{-8}-10^{-4}$ cm^{-1}). A large tunneling gap results from a high-range extradiagonal parameter that mixes $+M_J$ with $-M_J$ in the ground state, either directly or by means of an intermediate M_J. In turn, large extradiagonal parameters can often be related to molecular high-symmetry axes. Hence, for the design of molecules with large tunneling gaps, we will need to have a M_J ground-state doublet that can be mixed by an extradiagonal term allowed by the symmetry of the molecule. Let us give two examples based on POM chemistry. The first concerns the series **1** with D_{4d} symmetry, which we mentioned earlier. In this case, the small distortion from an ideal D_{4d} symmetry allows the appearance of terms B_4^4 and B_6^4. This should facilitate the mixing

dx.doi.org/10.1021/ic302068c | *Inorg. Chem.* 2012, 51, 12565−12574

of a ground-state doublet containing $M_J = \pm 4$, which is exactly what happens for the holmium derivative, as can be seen in Table 1. For this compound, long coherence times have been detected.[36] The second example involves the Preyssler POM anion $[LnW_{30}O_{110}]^{12-}$. This anion shows an atypical geometry with a C_5 axis in such a way that a very high B_6^5 extradiagonal parameter can be estimated. Therefore, when the ground state contains a doublet with $M_J = \pm 5$, a very strong mixing through $M_J = 0$ is possible. This situation may occur for the terbium derivative, which, according to our calculations, should lead to a tunneling gap $\Delta > 2$ cm^{-1}.[37]

Last but not least, one needs to consider interactions taking place beyond the first coordination sphere. The more relevant ones for our purposes are the interaction with other spins (electronic or nuclear) and electron−phonon coupling. In fact, a recent work shows that environmental decoherence[38] in a SMM model can be tracked down to precisely these three sources: magnons, nuclear spins, and phonons.[38]

Unwanted interaction with neighboring spin qubits is a common source of decoherence. In lanthanoid ions, this problem can be easily addressed by diamagnetic dilution. Of course, under certain conditions, spin−spin coupling can also be used as a resource instead of just as a problem. This has been exploited to implement an intramolecular Controlled-NOT quantum gate.[39]

Nuclear spins are best kept away from the spin qubit. When the nuclear spin belongs to the lanthanoid, it is strongly coupled to its electronic spin so that it does not introduce any decoherence. The most critical region is the close vicinity of the lanthanoid ion. That means that coordination by oxygen (or sulfur), which are nuclear-spin-free, is much preferred over coordination by nitrogen or halogens, which have nuclear spins. Carbon would be a good option, but in the vast majority of the cases, it is bonded to hydrogen, which has the highest gyromagnetic ratio of all elements. In fact, when ^{1}H is present in the sample, deuteration is often the most effective way to minimize decoherence.

Finally, we also need to understand and estimate the state-dependent electron−phonon coupling. Phonons can cause leakage to excited states within the same molecule, and they can communicate qubits at long distances even in the absence of dipolar coupling. The solution for this is to design qubits that are almost transparent to phonons, i.e., qubits in which the phonon interactions do not affect the energy differences within the qubit or the response to experimental stimuli. This, of course, can only be achieved after deep magnetostructural analysis. A general recipe would be to have a very rigid coordination sphere for the qubit, while the crystalline environment in which the qubit is embedded is much softer. This requirement is naturally satisfied by molecular-based materials.

CONCLUSIONS

Let us start by making a comparison between the polynuclear cluster-type SMMs and the mononuclear SIMs. In the former case, the two major goals have been (i) to increase through chemical design the superparamagnetic barrier and, consequently, the blocking temperature, and (ii) to study the quantum effects exhibited by these nanomagnets. In the case of the SIMs, owing to the large magnetic anisotropy of the rare earths, superparamagnetic barriers with energies on the order of, or higher than, k_BT are not unusual. Still, at low temperatures, the spin relaxation of these systems has shown to be often dominated by a fast quantum tunneling, thus preventing their use as magnetic memories (classical spin bits). In fact, the quantum effects in the SIMs are much more pronounced than those in the polynuclear cluster-type SMMs. Hence, in this class of nanomagnets, the major focus of interest will deal with the study of quantum phenomena like tunneling, relaxation, and coherence. In this context, these simple molecules are better suited for their integration as reliable quantum bits (qubits) for quantum computing than the polynuclear SMMs are. The reason lies in the larger stability of SIMs against decoherence because the robustness of a quantum state decreases with the system's number of degrees of freedom. This idea is further supported by the possibility of chemically controlling the quantum coherence in these systems. Thus, the main sources of decoherence, namely, the dipolar spin−spin and hyperfine interactions, can be easily minimized by magnetic dilution, i.e., the synthesis of crystals containing both magnetic and nonmagnetic molecules, and by the preparation of nuclear-spin-free molecules.

In this work, we have shown that the major electronic features that determine the spin dynamics of SIMs based on lanthanoids can be directly correlated with the local coordination environment around the f metal ion. By using a relatively simple point-charge model, we have shown that the splitting of the ground state, J, of the lanthanoid into M_J sublevels, caused by the presence of the CF created by the surrounding ligands, is in good agreement with that experimentally calculated through a fit of the magnetic data. The power of this approach is that it allows us to predict the energy splitting as well as the nature of the resulting wave functions of a lanthanoid complex in any environment, in terms of the CF parameters. At this point, it is important to notice that, in the case of f electrons, the high-order CF terms arise from interaction between the electic field and ground state J, whereas for d-transition-metal SMMs, they appear as perturbative corrections. This difference underlines the key influence of these CF parameters on the magnetic properties of lantanoid complexes. Our method refines a purely electrostatic model through shielding corrections and has been applied to examine the most common lanthanoid geometries: square antiprism, trigonal prism, and triangular dodecahedron. Several real lanthanoid-based SIMs have been studied, and general magnetostructural correlations have been proposed. Also, we have illustrated the use of DFT calculations to extend such an electrostatic model to organometallic SIMs exhibiting marked covalency effects.

Let us now summarize the main rules that need to be known for the design of a SIM.

(i) As a general rule, SIMs require a high M_J ground state, to create an energy barrier leading to slow spin relaxation, and low mixing in the wave functions, to minimize fast spin relaxation through quantum tunneling processes. In the simplest case, this can be achieved with an ideal pseudoaxial symmetry such as D_{4d}, C_{5h}, D_{6d}, or any symmetry of order 7 or higher (such as, for example, in organometallic sandwich-type complexes). In all of these symmetries, the most suitable case is achieved when the second-order uniaxial anisotropy, accounted for by the B_2^0 parameter (also known as D), is maximized. Depending on the metal, this favorable situation can be reached by increasing the electron density either near the uniaxial axis (in the case of Tb, Dy, and Ho) or near the basal plane (in the particular case of Er but also for Tm and Yb). Notice that the chemical inequivalence of the ligands or chelating groups needs to be

taken into account because it will usually lower the overall symmetry. So, the first condition requires an axial coordination sphere around the lanthanoid, exhibiting small deviations from the ideal symmetry in order to avoid an additional undesired mixing of the M_J ground state.

(ii) Not all of the molecular symmetries are equally suited for favoring SIM behavior. For example, in the case of octacoordinated complexes, one can imagine either an antiprismatic D_{4d} symmetry or a cubic O_h symmetry. However, because the cubic coordination lacks second-order uniaxial anisotropy, B_2^0, this geometry is unfavorable to exhibit a large energy barrier for the magnetization reversal. On the contrary, an axially distorted D_{4d} symmetry has high B_2^0 values (either positive or negative), providing most of the known examples of SIMs. Thus, axially elongated sites are favorable for Tb^{3+}, Dy^{3+}, and Ho^{3+}, as exemplified by the double-decker bis-(phthalocyaninato) complexes, while axially compressed sites are favorable for Er^{3+}, as exemplified by POMs.

(iii) Not always does the presence of an extensive mixture of M_J values in the ground-state doublet lead to quantum tunneling. In fact, if the two wave functions do not present any overlap, relaxation through tunneling is forbidden. Additionally phonons allow transitions with $\Delta M_J = \pm 1$. For example, lanthanoid complexes exhibiting D_{2d} triangular dodecahedral geometry typically have extradiagonal CF terms of the type B_4^4 and B_6^4, whose values are higher than those of the diagonal terms. In some cases, the mixing generated by these terms, which involve functions with M_J values differing by 4 units, does not prevent the presence of an energy barrier.

For the rational design of molecular spin qubits, we have to exert control on two levels: the CF geometric effect and interaction with further electron spins, nuclear spins, and phonons. Interaction with the environment has already been commented on above. Let us now comment on the effect of the CF around the lanthanoid. Two minimal electronic features are required for having a spin qubit: (i) a controlled mixing of the wave functions in a well-defined level subset and (ii) sufficient isolation of this subset from the rest of the spectrum. These two requirements are the same as those needed for the design of SIMs. Hence, many SIMs will also be useful as spin qubits. Additionally, lanthanoid complexes can present a large tunneling gap in the ground state, Δ, which can minimize decoherence through nuclear spins.[40] In this sense, the tunneling gap in lanthanoid SIMs can be much higher than that exhibited by cluster-type SMMs (by a factor larger than 10^4). Hence, this favorable effect for minimizing decoherence is expected to be much more pronounced in the case of mononuclear SIMs. Taking into account this last effect, the three conditions that favor the design of a qubit will be (i) to use non-Kramers ions (for example, Tb or Ho), (ii) to choose a geometry for this lanthanoid allowing for a large extradiagonal CF term, and (iii) to have a $\pm M_J$ ground-state doublet such that $2M_J$ is a multiple on the range of this extradiagonal operator, q. Because the q value coincides, in general, with the order of the main symmetry axis of the molecule, an easy way to satisfy the third requirement is to find a molecular geometry having a q-range axis equal to $2M_J$. Two examples that illustrate this point are provided by the POMs $[Ho(W_5O_{18})_2]^{9-}$ (C_{4v}, $M_J = \pm 4$, and $\Delta > 0.1$ cm^{-1})[50] and $[TbW_{30}O_{110}]^{12-}$ (C_{5v}, $M_J = \pm 5$, and $\Delta \approx 2$ cm^{-1}), both of which have been experimentally found to show unusually long decoherence times.

THEORETICAL BACKGROUND AND COMPUTATIONAL METHOD

We consider a CF Hamiltonian, $\hat{H}_{cf}$, which parametrizes the electric field effect caused by the surrounding ligands acting over the central ion. $\hat{H}_{cf}$ generated by a charge distribution can be written in its most primitive form as the sum of Coulomb fields created by the charges. In order to determine the CF parameters, we adopt the point-charge electrostatic model,[41,42] in which N ligands are represented by their point charges (Z_i). Because of our interest in the magnetic properties, all of the excited levels are neglected and we consider only the splitting of the ground-state J multiplet.[43]

$\hat{H}_{cf}$ can be expressed in terms of different operators: spherical harmonics,[44] Stevens' operators,[20] or irreducible tensor operators.[45] The different notational conventions of this Hamiltonian are related to each other by equivalence coefficients. In this article, we use the extended Stevens operators, O_q^k, which are the most extensively adopted operators in CF calculations.[46,47] For a given J multiplet, the CF Hamiltonian based on the Stevens formalism takes the general form

$$\hat{H}_{cf}(J) = \sum_{k=2,4,6} \sum_{q=-k}^{k} B_k^q O_k^q = \sum_{k=2,4,6} \sum_{q=-k}^{k} a_k(1-\sigma_k) A_k^q \langle r^k \rangle O_k^q \quad (1)$$

where k is order (also called rank or degree) of the Stevens operator equivalents O_k^q, and q is the operator range that varies between k and $-k$, a_k are the α, β, and γ Stevens coefficients for $k = 2$, 4, and 6, respectively, and σ_k are the Sternheimer shielding parameters of the 4f electronic shell and $\langle r^k \rangle$ are the moments of the 4f radial wave function.[48] α, β, and γ are tabulated and depend on the number off-electrons. Hence, the CF parameters A_k^q and B_k^q are referred to the ground state as well.

The CF parameters A_k^q can be calculated by the following expression:

$$A_k^q = \frac{4\pi}{2k+1} c_{kq} (-1)^q \sum_{i=1}^{N} \frac{Z_i e^2 Y_{k-q}(\theta_i, \phi_i)}{R_i^{k+1}} \quad (2)$$

where R_i, θ_i, and φ_i are the effective polar coordinates of the point charge and Z_i is the effective point charge, associated to the i-th ligand with the lanthanoid at the origin; e is the electron charge and c_{kq} is a tabulated numerical factor that relates spherical harmonics Y_{k-q} and Stevens operator equivalents. Note that, unless otherwise specified, Y_{kq}, A_k^q, and B_k^q are complex numbers. Because they have the same angular nodes, they can sometimes be used interchangeably. We use Y_{kq} to designate the mathematical shapes, A_k^q to discuss the field created by a set of ligands, and B_k^q for the final CF parameters.

This model has been implemented in a freely distributable computational code,[49] which has been used throughout this paper. The code, called SIMPRE, is written in portable Fortran 77 and calculates the full set of CF parameters, energy levels, wave vectors, and wave functions, as well as the magnetic properties for a mononuclear lanthanoid complex. This facilitates magnetostructural studies on real and ideal complexes, allowing the fitting and prediction of the magnetic properties.

AUTHOR INFORMATION

Corresponding Author

*E-mail: eugenio.coronado@uv.es.

Notes

The authors declare no competing financial interest.

ACKNOWLEDGMENTS

The present work has been partly funded through the EU (Project ELFOS and ERC Advanced Grant SPINMOL), the Spanish MINECO (Grants MAT2007-61584 and 2011-22785 co-financed by Feder, and the CONSOLIDER project on

Molecular Nanoscience), the Generalitat Valenciana (Prometeo and ISIC Programmes). A.G.-A. acknowledges funding by Project ELFOS under Contract UV-CI-12-009. J.J.B. and S.C.-S. thank the Spanish MINECO for a FPU predoctoral grant. A.P. thanks the Universitat de Valencia for a visiting research grant.

REFERENCES

(1) (a) Thomas, L.; Lionti, F.; Ballou, R.; Gatteschi, D.; Sessoli, R.; Barbara, B. *Nature* **1996**, *383*, 145−147. (b) Friedman, J. R.; Sarachik, M. P.; Tejada, J.; Ziolo, R. *Phys. Rev. Lett.* **1996**, *76*, 3830−3833.
(2) Wernsdorfer, W.; Ohm, T.; Sangregorio, C.; Sessoli, R.; Mailly, D.; Paulsen, C. *Phys. Rev. Lett.* **1999**, *82*, 3903−3906.
(3) Gatteschi, D.; Sessoli, R. *Angew. Chem., Int. Ed.* **2003**, *42*, 268−297.
(4) (a) Ardavan, A.; Blundell, S. J. *J. Mater. Chem.* **2009**, *19*, 1754−1760. (b) Troiani, F.; Affronte, M. *Chem. Soc. Rev.* **2011**, *40*, 3119−3129. (c) Stamp, P. C. E.; Gaita-Ariño, A. *J. Mater. Chem.* **2009**, *19*, 1718−1730. (d) Lehmann, J.; Gaita-Ariño, A.; Coronado, E.; Loss, D. *Nat. Nanotechnol.* **2007**, *2*, 312−317.
(5) Sessoli, R.; Tsai, H. L.; Schake, A. R.; Wang, S.; Vincent, J. B.; Folting, K.; Gatteschi, D.; Christou, G.; Hendrickson, D. N. *J. Am. Chem. Soc.* **1993**, *115*, 1804−1816.
(6) (a) Lin, P. H.; Burchell, T. J.; Ungur, L.; Chibotaru, L. F.; Wernsdorfer, W.; Murugesu, M. *Angew. Chem., Int. Ed.* **2009**, *48*, 9489−9492. (b) Guo, Y. N.; Xu, G. F.; Gamez, P.; Zhao, L.; Lin, S. Y.; Deng, R.; Tang, J.; Zhang, H. J. *J. Am. Chem. Soc.* **2010**, *132*, 8538−8539. (c) Rinehart, J. D.; Fang, M.; Evans, W. J.; Long, J. R. *Nat. Chem.* **2011**, *3*, 538−542. (d) Hewitt, I. J.; Tang, J.; Madhu, N. T.; Anson, C. E.; Lan, Y.; Luzon, J.; Etienne, M.; Sessoli, R.; Powell, A. K. *Angew. Chem., Int. Ed.* **2010**, *49*, 6352−6356. (e) Car, P. E.; Perfetti, M.; Mannini, M.; Favre, A.; Caneschi, A.; Sessoli, R. *Chem. Commun.* **2011**, *47*, 3751−3753. (f) Sessoli, R.; Powell, A. K. *Coord. Chem. Rev.* **2009**, *253*, 2328−2341.
(7) Sorace, L.; Benelli, C.; Gatteschi, D. *Chem. Soc. Rev.* **2011**, *40*, 3092−3104.
(8) Ishikawa, N.; Sugita, M.; Ishikawa, T.; Koshihara, S. Y.; Kaizu, Y. *J. Am. Chem. Soc.* **2003**, *125*, 8694−8695.
(9) (a) AlDamen, M. A.; Clemente Juan, J.; Coronado, E.; Martí-Gastaldo, C.; Gaita-Ariño, A. *J. Am. Chem. Soc.* **2008**, *130*, 8874−8875. (b) Aldamen, M. A.; Cardona-Serra, S.; Clemente-Juan, J. M.; Coronado, E.; Gaita-Ariño, A.; Martí-Gastaldo, C.; Luis, F.; Montero, O. *Inorg. Chem.* **2009**, *48*, 3467−3479.
(10) Jiang, S.; Wang, B.; Sun, H.; Wang, Z.; Gao, S. *J. Am. Chem. Soc.* **2011**, *133*, 4730−4733.
(11) Jiang, S.; Wang, B.; Su, G.; Wang, Z.; Gao, S. *Angew. Chem., Int. Ed.* **2010**, *49*, 7448−7451.
(12) (a) Car, P. E.; Perfetti, M.; Mannini, M.; Favre, A.; Caneschi, A.; Sessoli, R. *Chem. Commun.* **2011**, *47*, 3751−3753. (b) Cucinotta, G.; Perfetti, M.; Luzon, J.; Etienne, M.; Car, P. E.; Caneschi, A.; Calvez, G.; Bernot, K.; Sessoli, R. *Angew. Chem., Int. Ed.* **2012**, *51*, 1606−1610.
(13) (a) Rinehart, J. D.; Long, J. R. *J. Am. Chem. Soc.* **2009**, *131*, 12558−12559. (b) Rinehart, J. D.; Meihaus, K. R.; Long, J. R. *J. Am. Chem. Soc.* **2010**, *132*, 7572−7573.
(14) Harman, W. H.; Harris, T. D.; Freedman, D. E.; Fong, H.; Chang, A.; Rinehart, J. D.; Ozarowski, A.; Sougrati, M. T.; Grandjean, F.; Long, G. J.; Long, J. R.; Chang, C. J. *J. Am. Chem. Soc.* **2010**, *132*, 18115−18126.
(15) Zadrozny, J. M.; Long, J. R. *J. Am. Chem. Soc.* **2011**, *133*, 20732−20734.
(16) Bertaina, S.; Gambarelli, S.; Tkachuk, A.; Kurkin, I. N.; Malkin, B.; Stepanov, A.; Barbara, B. *Nat. Nanotechnol.* **2007**, *2*, 39.
(17) Giraud, R.; Wernsdorfer, W.; Tkachuk, A. M.; Mailly, D.; Barbara, B. *Phys. Rev. Lett.* **2001**, *87*, 057203.
(18) Rinehart, J. D.; Long, J. R. *Chem. Sci.* **2011**, *2*, 2078−2085.
(19) Stevens, K. W. H. *Proc. Phys. Soc. A* **1952**, *65*, 209−215.
(20) (a) Ishikawa, N.; Sugita, M.; Wernsdorfer, W. *Angew. Chem., Int. Ed.* **2005**, *44*, 2931−2935. (b) Ishikawa, N.; Sugita, M.; Wernsdorfer, W. *J. Am. Chem. Soc.* **2005**, *127*, 3650−3651.
(21) Barsukova, M.; Izarova, N. V.; Biboum, R. N.; Keita, B.; Nadjo, L.; Ramachandran, V.; Dalal, N. S.; Antonova, N. S.; Carbó, J. J.; Poblet, J. M.; Kortz, U. *Chem.—Eur. J.* **2010**, *16*, 9076−9085.
(22) Kortz, U.; Coronado, E. et al. Unpublished results.
(23) Ishikawa, N.; Sugita, M.; Okubo, T.; Takana, N.; Iino, T.; Kaizu, Y. *Inorg. Chem.* **2003**, *42*, 2440−2446.
(24) Alvarez, S.; Alemany, P.; Casanova, D.; Cibera, J.; Llunell, M.; Avnir, O. *Coord. Chem. Rev.* **2005**, *249*, 1693−1708.
(25) Bernal, E. G. *J. Chem. Phys.* **1971**, *55*, 2538−2549.
(26) Coronado, E.; Giménez-Saiz, C.; Recuenco, A.; Tarazón, A.; Romero, F. M.; Camón, A.; Luis, F. *Inorg. Chem.* **2011**, *50*, 7370−7372.
(27) Pointillart, F.; Klementieva, S.; Kuropatov, V.; Le Gal, Y.; Golhen, S.; Cador, O.; Cherkasovb, V.; Ouahab, L. *Chem. Commun.* **2012**, *48*, 714−716.
(28) Li, D.-P.; Wang, T.-W.; Li, C.-H.; Liu, D.-S.; Li, Y.-Z.; You, X.-Z. *Chem. Commun.* **2010**, *46*, 2929−2931.
(29) (a) Rinehart, J. D.; Long, J. R. *J. Am. Chem. Soc.* **2009**, *131*, 12558−12559. (b) Maria, L.; Campello, M. P.; Domingos, A.; Santos, I.; Andersen, R. *Dalton Trans.* **1999**, *43*, 2015. (c) Rinehart, J. D.; Meihauss, K. R.; Long, J. R. *J. Am. Chem. Soc.* **2010**, *132*, 7572. (d) Antunes, M. A.; Pereira, L. C. J.; Santos, I. C.; Mazzanti, M.; Marçalo, J.; Almeida, M. *Inorg. Chem.* **2011**, *50*, 9915. (e) Magnani, N.; Apostolidis, C.; Morgenstern, A.; Colineau, E.; Griveau, J. C.; Bolvin, H.; Walter, O.; Caciuffo, R. *Angew. Chem., Int. Ed.* **2011**, *50*, 1696. (f) Rinehart, J. D.; Long, J. R. *Dalton Trans.* **2012**, DOI: 10.1039/c2dt31352a. (g) Sun, Y.; McDonald, R.; Takats, J..; Day, V. W.; Eberspacher, T. A. *Inorg. Chem.* **1994**, *33*, 4433. (h) Coutinho, J. T.; Antunes, M. A.; Pereira, L. C. J.; Bolvin, H.; Marçalo, J.; Mazzanti, M.; Almeida, M. *Dalton Trans.* **2012**, DOI: 10.1039/c2dt31421e. (i) Magnani, N.; Colineau, E.; Eloirdi, R.; Griveau, J.-C.; Caciuffo, R.; Cornet, S. M.; May, I.; Sharrad, C. A.; Collison, D.; Winpenny, R. E. P. *Phys. Rev. Lett.* **2010**, *104*, 197202. (j) Mills, D. P.; Moro, F.; McMaster, J.; Van Slageren, J.; Lewis, W.; Blake, A. J.; Liddle, S. T. *Nat. Chem.* **2011**, *3*, 454.
(30) Baldoví, J. J.; Cardona-Serra, S.; Clemente-Juan, J. M.; Coronado, E.; Gaita-Ariño, A. In press.
(31) Palii, A. V.; Clemente-Juan, J. M.; Coronado, E.; Klokishner, S. I.; Ostrovsky, S. M.; Reu, O. S. *Inorg. Chem.* **2010**, *49*, 8073−8077.
(32) (a) Morrison, C. A. Lectures on Crystal Field Theory, HDL-SR-82-2, Harry Diamond Laboratories Report, 1982. (b) Porcher, P.; Dos Santos, M. C.; Malta, O. *Phys. Chem. Chem. Phys.* **1999**, *1*, 397.
(33) (a) Malkin, B. Z. Crystal field and electron−phonon interaction in rare-earth ionic paramagnets. In *Spectroscopy of Solids Containing Rare-Earth Ions*; Kaplyanskii, A. A., Macfarlane, R. M., Eds.; North-Holland: Amsterdam, The Netherlands, 1987; p 13. (b) Popova, M. N.; Chukalina, E. P.; Malkin, B. Z.; Saikin, S. K. *Phys. Rev. B* **2000**, *61*, 7421−7427. (c) Klokishner, S. I.; Ostrovsky, S. M.; Reu, O. S.; Palii, A. V.; Tregenna-Piggott, P. L. W.; Brock-Nannestad, T.; Bendix, J.; Mutka, H. *J. Phys. Chem. C* **2009**, *113*, 8573−8582.
(34) Fuchs, G. D.; Burkard, G.; Klimov, P. V.; Awschalom, D. D. *Nat. Phys.* **2011**, *7*, 789−793.
(35) Palii, A.; Tsukerblat, B.; Clemente-Juan, J. M.; Gaita-Ariño, A.; Coronado, E. *Phys. Rev. B* **2011**, *84*, 184426.
(36) Hill, S.; Coronado, E.; et al. Unpublished results.
(37) Cardona-Serra, S.; Clemente-Juan, J. M.; Coronado, E.; Gaita-Ariño, A.; Camón, A.; Evangelisti, M.; Luis, F.; Martínez-Pérez, M. J.; Sesé, J. *J. Am. Chem. Soc.* **2012**, *134*, 14982−14990.
(38) (a) Takahashi, S.; Tupitsyn, I. S.; van Tol, J.; Beedle, C. C.; Hendrickson, D. N.; Stamp, P. C. E. *Nature* **2011**, *476*, 76−79. (b) Stamp, P. C. E. *Phil. Trans. R. Soc. A.* **2012**, *370*, 4429−4453.
(39) Luis, F.; Repollés, A.; Martínez-Pérez, M. J.; Aguilá, D.; Roubeau, O.; Zueco, D.; Alonso, P. J.; Evangelisti, M.; Camón, A.; Sesé, J.; Barrios, L. A.; Aromí, G. *Phys. Rev. Lett.* **2011**, *107*, 117203.
(40) Stamp, P. C. E.; Tupitsyn, I. S. *Phys. Rev. B* **2004**, *69*, 014401.
(41) Hutchings, M. T. *Solid State Phys.* **1964**, *16*, 227−273.

(42) Figgis, B. W. *Introduction to ligand fields*; Wiley-Interscience: New York, 1966.
(43) Kahn, O. *Molecular Magnetism*; Wiley-VCH: Weinheim, Germany, 1993.
(44) Elliott, R. J.; Stevens, K. W. H. *Proc. R. Soc., Ser. A* **1952**, *215*, 437−453.
(45) Morrison, C. A.; Wortman, D. E.; Karayianis, N. *J. Phys. C: Solid State Phys.* **1976**, *9*, L191−194.
(46) (a) Buckmaster, H. A. *Can. J. Phys.* **1962**, *40*, 1670−1677. (b) Rudowicz, C. *J. Phys. C: Solid State Phys.* **1985**, *18*, 1415−1430.
(47) (a) Ryabov, I. D. *J. Magn. Reson.* **1999**, *140*, 141. (b) Ryabov, I. D. *Appl. Magn. Reson.* **2009**, *35*, 481−494.
(48) Edvarsson, S.; Klintenberg, M. *J. Alloys Compd.* **1998**, *275*−*277*, 230−233.
(49) Baldoví, J. J.; Cardona-Serra, S.; Clemente-Juan, J. M.; Coronado, E.; Gaita-Ariño, A.; Palii, A. To be submitted.
(50) Ghosh, S.; Datta, S.; Friend, L.; Cardona-Serra, S.; Gaita-Ariño, A.; Coronado, E.; Hill, S. *Dalton Trans.* **2012**, DOI: 10.1039/C2DT31674A.
(51) Baldoví, J. J.; Borrás-Almenar, J. J.; Clemente-Juan, J. M.; Coronado, E.; Gaita-Ariño, A. *Dalton Trans.* **2012**, DOI: 10.1039/C2DT31411H.